Mechanics of Soft Tissue Reactions to Textile Mesh Implants

Aroj Bhattarai and Manfred Staat

1 Introduction

Prosthetic or surgical meshes are permanently implanted inside the body to repair hernia and urogynecological disorders such as pelvic organ prolapse (POP) and incontinence that occurs due to weakened/damaged supporting tissues. After the first ever design of the polypropylene surgical mesh to repair abdominal hernia in the late 1950s [83], a novel use of biological materials convincingly reduced the rate of recurrence (less than 10%) compared to the conventional suture technique with 50% recurrence rate [14, 76]. Eventually, in the 1970s, surgeons began inserting surgical meshes to correct POP and stress urinary incontinence also. Advanced research in the last 50 years on the repair of abdominal wall hernia and pelvic floor dysfunctions has achieved significant improvements in the reconstruction techniques and a rapid growth in varieties of prosthetic meshes. Today, it is estimated that more than 200 different textile constructs are available with variations in polymer and pore structure [46] and more than 20 million meshes are implanted per year world-wide [9, 72].

In initial days of hernia repair, the prosthetic meshes constructed from stronger material such as polypropylene were popularly used due to their excellent biocompatibility, lowest failure rates, improved tolerance to bacterial infection and good cost/benefits of the polymer [1]. Such early mesh constructions were heavy weight with small pore size and larger mesh area. Over the years, despite clinical success, numerous post-operation complications were reported later with such implantations in the form of strong foreign body reaction such as inflammatory

A. Bhattarai (✉) · M. Staat
Biomechanics Laboratory, Institute for Bioengineering, University of Applied Sciences Aachen, Heinrich-Mußmann-Str. 1, 52428 Jülich, Germany
e-mail: Bhattarai@fh-aachen.de

G. M. Artmann et al. (eds.), *Biological, Physical and Technical Basics of Cell Engineering*, https://doi.org/10.1007/978-981-10-7904-7_11

reaction [13, 62], larger mesh shrinkage [3] and adhesion formation to adjacent viscera [54, 84] that ultimately affected the healing process [17, 18]. However, symptoms varied for several reasons in character and severity from patient to patient. Native tissue compliance loss with excessively stiff, dense, heavy and small pore mesh were also found [85]. Mesh shrinkage [3], scar tissue formation [85] and mechanical mismatch between native abdominal tissue and prosthesis [6, 24] were found to be the reason for recurrence, treatment failure that forces complete removal of the implant from the body. Early meshes with high mesh stiffness were also related to the likelihood of post-operative pain, unnatural or difficult organ movements, central mesh ruptures and biomechanical and biological degeneration of host tissue as erosion and exposure [3, 21, 26, 27, 52, 58].

Over the seven-year period between 1997 and 2005, influence of mesh weight and mesh porosity were identified to be decisive for biocompatibility and stabilization of the surgical treatment [2, 46, 50]. The concept have been widely accepted among surgeons and manufacturers that systematically updated the mesh design changing polymer type (polytetrafluroethylene (PTFE), polyethylene terephthalate (PET, PETE), expanded PTFE and polyvinylidene fluoride (PVDF)), pore size, pore geometry and biocompatibility of the mesh implants [20, 42]. Clinical trials showed the superiority of the light weight large porous textile constructions with significantly improved integration of the mesh into recipient tissues, decreased risk of bacterial colonization, reduced inflammation and fibrous reaction, and improved quality of life after repair [50, 51, 66, 68, 70]. Further in 2008, Mühl et al. [63] introduced the concept of effective porosity to characterize the textile porosity where large pore meshes preserves the effective porosity under deformation and avoids formation of scar bridges.

Mesh development is an ongoing process, a good mesh should optimally fulfill certain requirements, such as negligible foreign body reaction with no pathological fibrosis, flexibility with adaptable stiffness, adequate adhesion especially near the sutures, and mesh dynamics close to the anisotropic host tissue. Since, every prosthesis possess different mechanical properties, the response to the native tissues varies hugely making it difficult for surgeons to select the most appropriate mesh and its orientation for each type of patient with each type of disorder. To achieve a physiological behavior of the implanted mesh in the body, engineers and manufacturers should be aware of how the host tissue would respond with the implantation of such biomaterials. This chapter reviews some mesh related complications arising from the mechanical behavior of the mesh implants. Standard protocols for uniaxial tensile test in orthogonal symmetry directions are used to characterize the compressible dry meshes. The characterization should help predict how well a surgical mesh may contribute to the short-term and long-term success of the repair for hernia and urogynecological disorders.

2 Prosthetic Meshes

Biologically and mechanically competent tissue-mesh response is a key factor in repairing herniation and pelvic floor dysfunctions. An ideal synthetic mesh should always provide structural support to the organs, restore anatomical function and treat physiological disorders with post-operation complications as less as possible. In order to achieve idealistic functionality and biological compatibility of prosthetic implants, properties of (type, dimensions and mechanics) polymer and (size and deformation under force) pores should be carefully understood.

2.1 Textile Structures

Textile constructions can be monofilament or multifilament. Common monofilament meshes are very distensible, have thicker fibrils (100–150 μm) and large pore whereas, most multifilament meshes are softer, less distensible with thinner fibrils (20–30 μm) and smaller pores. Due to less inter-fiber space, multifilament meshes do not allow macrophages and neutrophils to enter through small pores. This provides comfortable environment for bacteria to survive within pores making such meshes at highest risk of infection.

2.2 Textile Porosity

Porosity is defined as the ratio of open space relative to the total area of the textile. It is an important parameter to predict the biocompatibility of the synthetic meshes. During the healing stage, granulomas are formed around mesh fibers as part of the foreign body reaction that become confluent with each other and encapsulate the entire mesh. A stiff scar plate is formed which reduces the mesh flexibility [38]. Mühl et al. introduced the concept of effective porosity that considers only the scar free or open pores [63]. Effective porosity excludes all pores, which are smaller in diameter than a critical diameter which depends on the mesh material, 1 mm for Polypropylene (PP) mesh and 0.6 mm for polyvinyldene fluoride (PVDF) [22, 63, 66]. Meshes with large pores preserve effective porosity and exhibit less inflammatory infiltrate, connective tissue, fistula formation, calcification and scar bridging, which allows increased soft tissue ingrowth.

2.3 An Ideal Polymer: Polyvinvlidene Versus Polypropylene?

Mechanically, an ideal synthetic mesh can be obtained from a mono filamentous large porous structure with anisotropic mechanical properties that mimics the mechanics of the host tissue. However, the biochemical compatibility of the meshes can be achieved through the choice of appropriate polymer material that affects the inflammatory response with granuloma formation. PP and PVDF are the mostly used polymers to construct surgical meshes due to their lesser amount of foreign body reaction compared to other available polymers. Though, PP shows inert response during infection, have excellent capacity for integration and are low cost meshes tested for years [55], they results in an intensified inflammatory reaction characterized by pronounced foreign body granuloma and are less stable. On the other hand, PVDF filaments have excellent biocompatibility and reduced adverse foreign body reaction, such as scar formation or pain claiming a higher biocompatibility and biostability than polypropylene [49]. A PVDF meshes has been successfully used as composite scaffold for cell cultures [25]. Some long-term advantages of the PVDF meshes against PP meshes are (a) no mesh curling under stress [66], (b) durability (lesser loss of tensile strength due to hydrolysis against PP: 7.5% vs. 46.6%) [53], (c) reduced risk of infection due to lower bacterial adherence, and (d) reduced mesh erosion [43].

3 Mechanics of Different Textiles

3.1 Specimen Preparation

Three different DynaMesh® meshes SIS direct soft (SD), CICAT and PRS soft (PRS) from FEG Textiltechnik mbH, Aachen, Germany have been tested. All of the selected meshes are monofilament made out of PVDF polymer but have a considerably different structure constructed for specific applications: SD is used for the repair of stress urinary incontinence, CICAT for abdominal hernia repair and PRS is used for uterine/vaginal vault prolapse correction. Numerous mechanical tests have been standardized to characterize the mechanical behavior of an anisotropic mesh materials. Among them, most common test are uniaxial tensile test, biaxial tensile test, shear test and inflation test.

For uniaxial tensile tests specimens (70 mm × 30 mm) were cut out of each mesh in longitudinal direction and transverse direction with respect to knitted pattern. The thickness and the pore size was measured using a digital microscope VHX-600 (Keyence, Japan). For inflation test, mesh specimen of 50 mm × 50 mm were cut and placed between two PVC plastic plates, see Fig. 1a. In [86] biaxial tests have been performed to characterize the passive behavior of the abdominal wall under three configurations: intact, after creating a defect simulating an

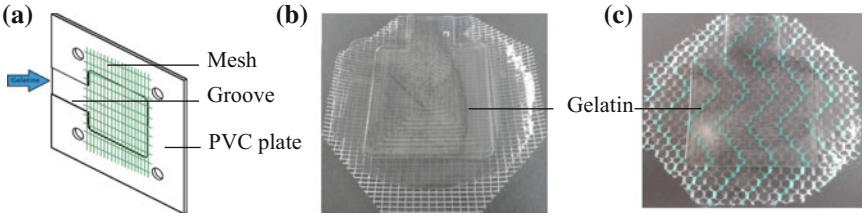

Fig. 1 Mesh specimen preparation for inflation (bulge) test: **a** schematic drawing of PVC plastic plate and mesh; **b** Dynamesh-PRS soft specimen with gelatin; **c** Dynamesh-CICAT specimen with transparent gelatin

incisional hernia, and after a repair with a mesh implanted intraperitonally. As alternative to animal testing ballistic gelatin type 3 of GELITA® (Eberbach, Germany), as a soft tissue surrogate was then poured inside the groove (1 mm deep), when cooled it forms a flexible gelatin-mesh complex (GMC), as shown in Fig. 1b, c. Gelatin has the practical advantage that its transparency and photoelastcity show detailed local behavior.

3.2 Mechanical Test Set Up

The uniaxial tensile tests are performed on a tension testing machine Z 010 (Zwick Roell AG, Ulm, Germany). Two uniaxial tests protocols are followed on dry mesh and explants (dry mesh and ballistic gelatin). The two ends of the testing meshes are clamped properly at a distance of 50 mm, see Fig. 2a. For strong grip and to protect the mesh against cutting by the fixation, paper or PVC foils are used. Digital image correlation (DIC) technique is used to measure the stretch during tests that is based on the optical measurement of the deformation of a speckle pattern made by grey graphite spray. The camera has taken pictures during the test with a frequency of 1 Hz for DIC and the deformation is analyzed with the software ISTRA 4D (Limess Messtechnik und Software GmbH, Krefeld, Germany) using a correlation algorithm.

Figure 2b shows second setup of biaxial test. GMC is clamped airtightly between two 2 mm thick stainless steel plates. Two cameras (uEye Modell UI-122xLE, WVGA (752 × 480); Fujinon lens HF25HA-1B) at two orthogonal observation planes measures the profile movement of the inflating GMC and captures the deformation of the anisotropic mesh. At the same time, air is blown to generate pressure inside the GMC that is measured by the pressure transducer. An automation program LabView (National Instruments, Austin, Texas) elaborates images with the predefined algorithm. The height of the inflated GMC was measured before gelatin layer bursts. Engineering parameters such as stress and strain are computed to evaluate the mechanical response of the GMC that can be compared with the in vivo response of the tissue-mesh complex.

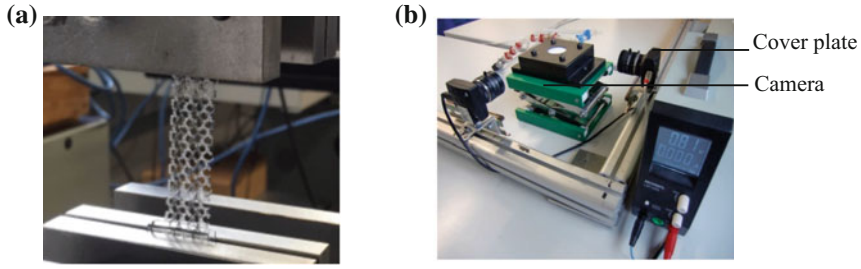

Fig. 2 Synthetic mesh clamped to **a** uniaxial tensile and **b** bulge test machines

3.3 Uniaxial Tensile Test on Rectangular Pore Dry Mesh

Uniaxial tensile tests on structurally similar dry PRS and SD mesh provided qualitatively similar results. As shown in Fig. 3b, c, the characteristic stress-stretch curves are nearly linear and orthotropic. Curves are plotted until complete failure of the implant. The SD mesh has larger toe stiffness and larger strain at inflection than the PRS mesh. Linear stiffness is measured that determines the strength and clinical effectiveness of the implantation. The initial Young's modulus in longitudinal direction of the PRS mesh ($E_L = 29.778$ MPa) is greater than for the SD mesh ($E_L = 26.73$ MPa), whereas, the initial transverse modulus is larger for the SD mesh ($E_T = 3.58$ MPa vs. $E_T = 1.919$ MPa). The meshes show nonlinear orthotropic behavior for which a polyconvex hyperelastic material model has been successfully identified in [36]. For simplicity we continue here to discuss the stiffness only linearly.

On the other hand, the CICAT mesh with hexagonal pore shape shows highly nonlinear mechanical behavior under uniaxial tensile test, see Fig. 3a. Compared to stretched SD and PRS meshes in longitudinal direction, CICAT mesh possessed the largest toe region and lower stiffness (E = 13.207 MPa) in the linear region.

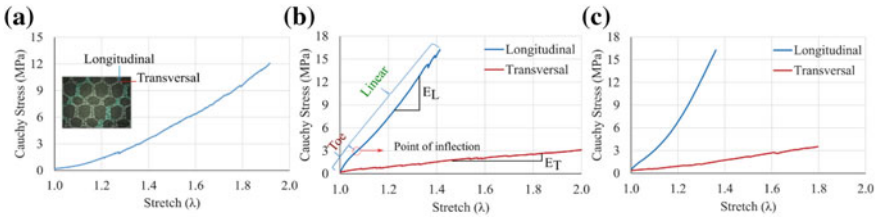

Fig. 3 Average stress-stretch curves of different dry meshes loaded in longitudinal and transverse direction for different meshes: **a** CICAT; **b** SD; **c** PRS

3.4 Optical Strain Measurement

The traditional extensometer technique provides an average strain over the specimen gauge length. For accurate strain measurement over the whole area between extensometer probes, especially at positions of necking, DIC tracks the positions of the same physical points during test. Lagrangian strains and stretch for large deformation are calculated and visualized by the color scaling using DIC analyses which are later converted into stretches for suitable presentation of results. In addition, for orthotropic prosthetic meshes, DIC technique benefits to measure the change of mesh porosity during tests.

3.4.1 SIS Direct Soft Mesh

In this part, the experiment performed using the DIC technique on the SIS direct soft mesh is presented. Two pairs of images at zero load and maximum load before failure of the mesh are compared when stretched in two orthogonal directions, see Fig. 4. Due to lesser number of woven fibers along transverse direction, axial elongation and transverse contraction of the specimen is significant. As shown in Fig. 4a, the textile construct shows a wide range of nearly linear stress-stretch curves when subjected to tension in longitudinal (E_L = 105.78 MPa) and transverse direction (E_T = 10.87 MPa). The dry meshes are found to be compressible with significant volume change during tensile test.

The stress-stretch behavior using uniaxial tensile test are qualitatively similar to that of DIC technique. However, computing Lagrangian strain and later converted into true strain and expressing them in terms of stretch reveals the maximum true stress is significantly large, see Figs. 3b and 4a. Under uniaxial tension load applied in longitudinal and transverse direction, the rectangular pore of the SD mesh becomes progressively bigger with increased fiber stretch. Stretching up to a stretch of λ = 1.4 in longitudinal direction, an increase in porosity of 2.4% was measured, see Fig. 4b. Despite of significant mesh contraction and higher stretchability near about 2, loading along transverse direction rather increases the mesh porosity by 3.93%.

3.4.2 Hernia Mesh

The uniaxial tensile tests of a PVDF hernia mesh shows a nonlinear stress-stretch behavior when loaded in longitudinal and transverse direction, see Fig. 5. Due to hexagonal pore geometry, pore deformation is extreme in low load range. In both loading directions, increased length and reduced width of the specimen is observed. Figure 6 shows deformed mesh when stretched in the longitudinal and the transversal direction of the mesh. Longitudinal (Fig. 6a) and transverse Lagrangian strains (Fig. 6b) for loading along both directions are shown in Fig. 6. Ciritsis et al.

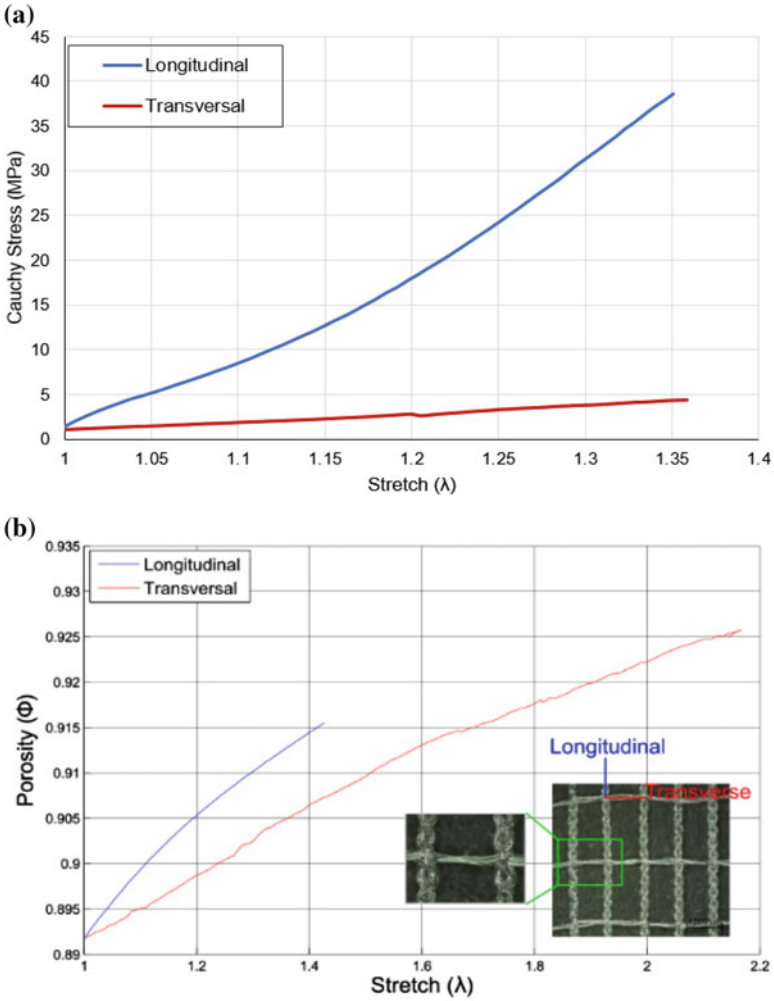

Fig. 4 Uniaxial tensile test on dry SD mesh using DIC technique; **a** the SD mesh elongates only by 40% if stretched to the thicker fiber (longitudinal) direction. In contrast, if rotated by 90°, an elongation of almost 100% occurs; **b** change of mesh porosity

[19] performed uniaxial tensile tests on PVDF constructed hernia mesh with hexagonal pore shape. As per the study, the porosity decrease was found to be 10.4 and 7.2% to a minimum in longitudinal and transverse directions, respectively.

In vivo hernia meshes loaded in biaxial tension show the increased porosity. In animal experiment, this led to an improved maturity of the scar indicated by a higher I/III collagen ratio which allowed the mesh implant to adapt to remain more flexible within the abdominal wall [19]. With respect to scar formation the concept of effective porosity has been suggested which could be only measured ex vivo with

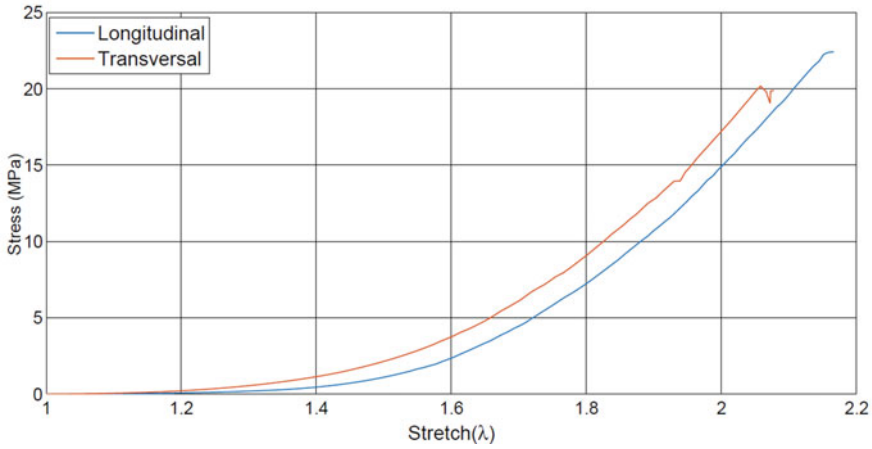

Fig. 5 Stress-stretch curves of anisotropic PVDF hernia mesh in uniaxial tensile test, see Fig. 2a

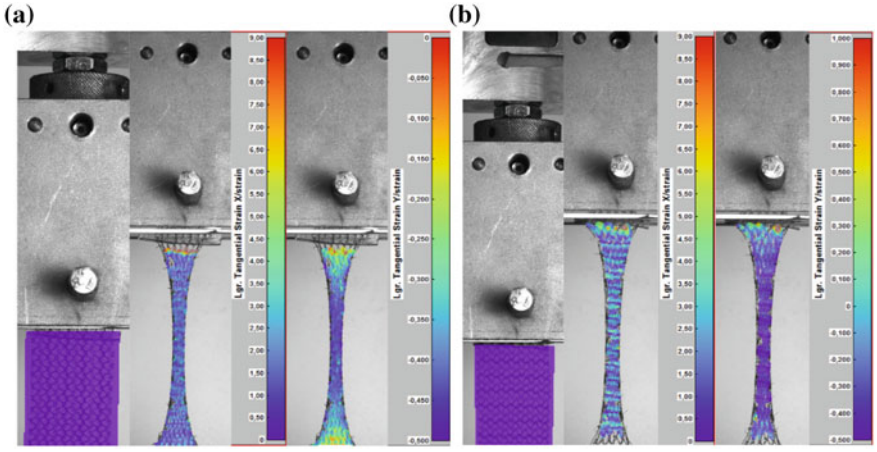

Fig. 6 **a** Lagrangian strains under loading in **b** longitudinal and **b** transverse fiber direction. Strain ε_x is extension in load direction and ε_y is contraction

a specially developed image processing. In [36] a new method has been presented which allows the calculation of effective pororsity from measurement of the global mesh deformation. Again the uniaxial tension was found to be critical because the pores collapse and effective porosity deceases to zero for the two tested meshes at stretches arround $\lambda = 1.4$.

3.5 *Photoelastic Uniaxial Tensile Test on Tissue Surrogate-Mesh Specimen*

The meshes are embedded in a transparent gelatin block that behaves similar to soft biological tissue but is transparent and photoelastic. Two ends of the mesh are clamped into a tension machine Z010 (Zwick Roell AG, Ulm, Germany). Applying tension to the gelatin-mesh complex (GMC) between two polarizing filters leads to isochromatic lines that represent lines of equal shear stresses. As shown in Fig. 7a, b, PRS mesh shows very little transverse contraction. However, due to axial force, the mesh surface is found to be increased by 18%. Since, there are no drastic reductions of the pore size, the mesh porosity and the effective porosity are satisfactorily preserved during uniaxial tensile test. Unlike PRS meshes, the CICAT mesh has different pore shapes in the loading direction and is completely unable to preserve its porosity; almost all pores are collapsed already under small tensile force, see Fig. 7c.

The failure modes of the tested meshes are observed from the photoelastic image of the uniaxial tension test that are quite distinct. The mesh shows a strong dependency of the GMC failure on the loaded direction. For the PRS soft mesh, loading along longitudinal direction sustains larger tensile force (124 N) that stresses the softer gelatin. The GMC specimen ruptures at lower stretch ($\lambda_{max} = 1.42$) whereas, along the transversal loading, the GMC is highly stretched ($\lambda_{max} = 2.05$). The zigzag (like steps of a staircase) orientation of transversal fiber families are unsupported at the boundaries and the mesh is pulled out at lower tensile load (22 N). This stresses the gelatin locally from where the rupture of the GMC begins, see Fig. 7b. On the other hand, the CICAT mesh with irregular hexagonal pores show large pore deformation along the loading direction. High shear stresses are generated in the gelatin at the boundaries of the mesh due to unequal stretching of the gelatin and the mesh, see Fig. 7c. Further stretching the

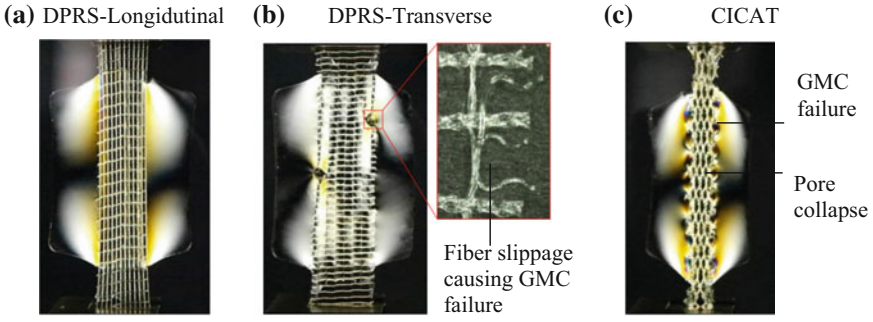

Fig. 7 Uniaxial tensile test on GMC specimen. DPRS mesh along **a** longitudinal direction (left: 80.89 N); **b** transverse direction (right: slippage of fiber (tearing out a seam) at less force, 15.89 N); **c** debonding of the CICAT mesh from the gelatin due to large transversal contraction and pore collapse at tensile force 60.404 N

GMC debonds the gelatin from the mesh along its edges and rupture of the GMC specimen occurs.

Such mesh edge failure have been observed after repair with the heavyweight small porous textiles [12] due to the heavy scar tissue formation, mesh shrinkage, mesh-size [50] and the mesh anisotropy [6]. However, pullout tensile tests and FE studies on monofilamentous and compliant Gynecare mesh (Ethicon, USA) shows a similar gradual debonding of the mesh from the tissue-surrogate gelatin in a zipper-like manner with huge pore deformation [31, 80]. Furthermore, large shear stresses at the lateral edges are generated when the mesh is highly stretched that is responsible for the failure of the compliant GC mesh. These reasons for similar mesh failure in two different classes of meshes are most likely due to the geometry, loading direction, compliance of the meshes and the generation of the normal and shear stresses.

3.6 Tissue Surrogate Mesh Failure Under Biaxial Inflation Test

Unlike, incontinence repair that supports mostly uniaxial physiological loads, abdominal hernia or pelvic organ prolapse repair uses a flat sheet of prosthetic meshes. They are designed to support the biaxial function of weak abdominal wall and pelvic organ and to restrain increased abdominal pressure on those surfaces developed with physical activities such as exercise, coughing, lifting, straining, and others. An inflation (bulge) test setup as shown in Fig. 2b on tissue surrogate gelatin-mesh complex theoretically mimics the physiological abdominal pressure and helps to determine the mechanical behavior after the implantation.

As shown in Fig. 8, the GMC specimen expands (inflates) with increased pressure from below. On the outer side of the GMC, small gelatin cups are formed across the mesh pores. Compliant CICAT-GMC specimen offers bigger cups due to (1.42 times in length and 2.41 times in width) larger pores than stiffer PRS-GMC specimen. The soft gelatin cups are highly stretched to burst at significantly lower pressure (97 kPa vs. 116 kPa) for CICAT-GMC specimen, thus failing at lower inflation height (6.89 mm vs. 11.44 mm), see Fig. 8a. For stiffer PRS mesh with small mesh pore the GMC bond is intact and bears larger stress. At high stress, the gelatin is scraped off from the edge of the cover plate to leak the pressure failing the GMC specimen. For inflation test, both meshes reveal materially linear response until failure and the structural differences of the meshes are found to be uninfluential. However, the maximum values of the principal stresses at the end of the experiment differ considerably in magnitude (483.79 MPa for CICAT and 1186.26 MPa for PRS). These differences are due to the pore geometry, pore size and the compliance of the two meshes.

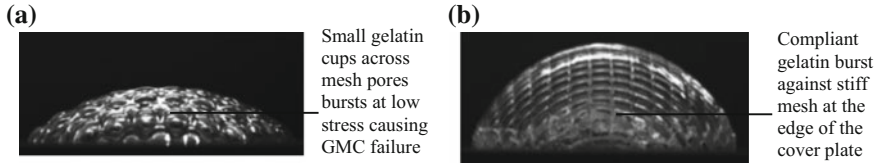

Fig. 8 Failure of tissue surrogate-mesh under biaxial inflation test: **a** Gelatin-CICAT mesh; **b** Gelatin-PRS mesh

3.7 Clinical Comparisons and Discussions

Immediately after implantation, biomaterials, such as prosthetic meshes are associated with the acute inflammation phase. Numerous blood and tissue proteins, such as cytokines or growth factors and leukocytes are deposited on the foreign body surface and injury site to form the provisional matrix and to clean the wound site [4, 40]. The types and concentration of such proteins are dependent on mesh surface properties and polymer hydrophilicity [87]. These proteins modulate the adhesion of monocytes/macrophages cells on the protein absorbed foreign object that are fused together to form larger foreign body giant cells (FBGCs) [16], also known as chronic inflammation. The chronic inflammation period for biocompatible materials should not be more than two weeks, otherwise may cause infection [5]. Adherent macrophages and FBGCs secrete fibroblast attractants, and the incoming fibroblasts from the surrounding tissue create an organized collagenous matrix around the biomaterial [78], called extracellular matrix (ECM) remodeling fibrosis. This vascular and collagenous capsule (usually 50–200 μm thick) isolates medical devices from the rest of the interstitial tissue at the end stage of wound healing process [86]. Later, abundant amount of fatty tissues and significantly less connective tissues penetrates completely into the pores of the mesh to form a layer of neo-tissue unit. But, why does the host tissue not heal normally around implants and what are the reasons for post-operation complications? These are very critical questions in surgical interventions for which thorough understanding of the foreign body response and the biocompatibility of the medical devices is important.

Biosafety (appropriate host response and in-growth of the patient's host tissue) and biofunctionality (effectiveness of biomaterial to further strengthen the defected area) are two elements to estimate the short-term and long-term biocompatibility and to predict post-operation complications and device failure/rejection [7]. In vivo assessment and cell culture examination are often performed to screen the tissue compatibility (toxicity) of implantable devices and to simulate the biochemical response of the host body [71, 73], the degree of which depends on the properties of the device, such as polymer composition, bacterial adhesion prior to surgery, smoothness and polymer surface area. However, biofunctionality (functional performance) of the mesh implants in vivo depends on the structural properties (effective porosity, pore size, pore deformation, filament type) and on the mechanical properties (tensile strength, isotropy, elasticity). A perfectly biocompatible mesh

material should provide maximum safety, match the behavior of the anisotropic host tissue and sufficient structural stability to physiological loadings; otherwise. Adverse effects are often observed in the form of chronic pain, infection, mesh shrinkage, scar formation and mesh rejection [3, 13, 21, 27, 52, 54, 58, 59, 62, 84, 85].

3.7.1 Mesh Complications

Inflammation

Almost all modern biomaterials trigger a wide variety of adverse responses in vivo mainly due to inflammation right after implantation [47]. The biosafety of the mesh implant is characterized by the inflammation phase: acute and chronic, that are associated with the deposition of proteins and macrophages/monocytes. Longer acute inflammation directly enhances the development of a greater amount of fibrous tissue, whereas, longer chronic inflammation initiates infection [5]. An ideal, biocompatible material is assumed to deposit thin fibrous tissue around the mesh filament and to fill sufficiently larger pores mainly by fat tissues [50] that maintains the elasticity of the mesh even after the inflammation phase. These animal experiments with a low-weight, large pore size and monofilament made mesh reduces the inflammation, maintains the flexibility of the mesh and provides greater host tissue mobility during physiological loadings [46].

In contrast, heavy-weight, multifilament made mesh with small pores increases the surface areas in contact with the recipient host tissue that basically aggravate the acute and chronic inflammatory phase. The adverse effects are seen in the form of (a) huge macrophages and FBGCs deposition at the interface, (b) intense fibrosis forming thicker connective tissue around filament, (c) poor or no fat cell penetration to the pore, and (d) disordered collagen metabolism with much lower collagen (I/III) ratio, see Fig. 9. Changes in this ratio affect both tensile strength and mechanical stability and may increase the risk of recurrence. This consequently forms a thick continuous connective tissue, also known as scar plate with tangled bundles of collagen fibers around the filaments which grow to the adjacent filaments [40, 63], a phenomena called ‘bridging’ [15]. This bridging of newly formed inter-filament connective tissue (stiff scar plate) as shown in Fig. 9 (a) prevents the pores to deform freely, (b) reduces the mesh compliance, (c) restricts the mobility of the host tissue, (d) prevents further tissue ingrowth and (d) finally causes recurrence. As a result, the healing of the wound may be retarded.

The polymer and fiber surface greatly affect the inflammatory response. PVDF made meshes result in a significantly reduced foreign body granuloma size [49] with reduced diameters of the inner (inflammatory infiltrate) and the outer (connective tissue infiltrate) ring of granulomas [39] compared to conventional PP (deposits more collagen, longer inflammation and scar neo-tissue) [8], and polyester mesh (long-lasting chronic inflammatory response) [65].

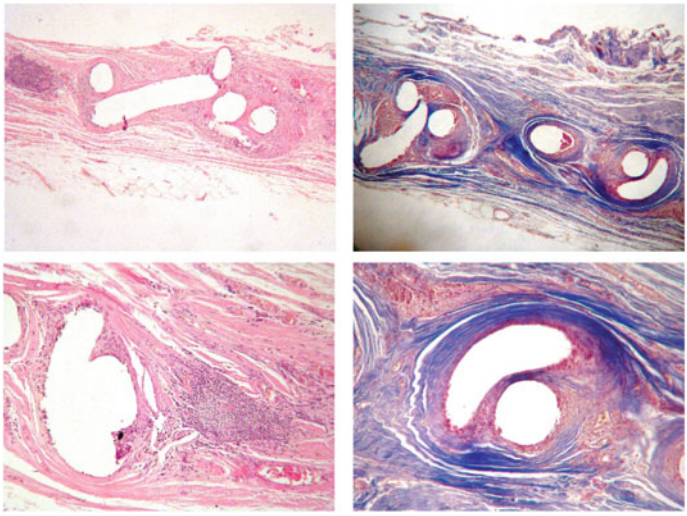

Fig. 9 Tissue response after suture repair. Histological analysis of explanted heavyweight polypropylene mesh stained with hematoxylin and eosin (H&E) or Masson's Trichrome. Histology reveals a large colony of leukocytes adjacent to the mesh filament and a thin layer of muscle surrounding the mesh filaments with an adjacent, dense layer of collagen surrounding the mesh filaments and is continuous between filaments 'bridging'. Images reprinted with permission courtesy of Melinda Harman, Ph.D. at Clemson University [15]

Seroma

Seroma is an ill-defined event, typically involving a collection of serous fluid in any potential fluid-occupying space that develops in the recipient body after surgery or any blunt injury. It usually appear under the surface of the skin as a swollen lump, like a large cyst when blood seeps out of the injured or ruptured blood vessels during operation. Seroma etiology remains unclear, its formation after incisional hernia repair with mesh is a most frequent problem due to local inflammatory response aggravated by the presence of the foreign body [10] and lasts for several weeks [81]. Chronic seromas are evidenced due to a long-term inflammatory reaction with heavyweight and small sized mesh monofilamentous PP and polyester meshes [46, 74].

Postoperative seroma formation anterior to mesh is very common up to 100% [35, 56, 81]; however, deep seroma behind the mesh develops an infection which ultimately requires surgical removal of the mesh [61, 77]. Further, a clear discharge of the serous fluid is non-harmful, however, bloody, colorful and odorous discharge indicates infection. Treatment options include observation for spontaneous resolution, percutaneous aspiration, closed suction drainage, abdominal binders, and sclerosant [57]. Though surgical drainage technique is used to prevent a seroma development and to reduce infection, seroma drainage and infection are inter-related. Drainage can introduce infection and in cases where the seroma causes

discomfort or is infected then drainage is required [33], thus, conservative follow up and microbiological examination is required.

Adhesion

Postsurgical adhesions are serious and frequent complication resulting in a similar way that a scar tissue forms and vary from filmy to dense [39]. Such adhesions occur in almost all meshes as a result of inflammation [12] containing multiple foreign body granulomas that connect tissues or anatomic structures to the textiles. Studies shows 20–80% of the subjects develop adhesions after ePTFE and PP mesh implantation [28, 60]. Other than the polymer type, factors associated with adhesion formation include trauma, tight suturing, thermal injury, infection and foreign bodies. Traditional heavy PP meshes with small pores induce an intense fibrotic reaction that produce dense adhesion around 62% of the mesh area and provide a strong adherence to the abdominal [12]. An anti-adhesion film-like barrier around the mesh filaments have been an alternate to reduce adhesions [12], however, light weight, large porous PVDF constructs with PP coating seem to be superior with regard to the induced intensity of inflammation and filmy adhesion of 34.6% mesh area that could be lysed with traction [39].

Collagen Metabolism

Collagen metabolism has an intense influence on the wound healing after mesh repair [48]; decreased ratio of collagen I to III increases the risk of hernia recurrences [41]. The inflammatory process after surgical implantation is accompanied by a pronounced fibrosis to deposit the fibrillary collagen molecule that are stabilized by intracellular hydroxylation reaction forming hydroxylysine and hydroxyproline [80]. Lysyl oxidase enzymes mediates a cross-linking process to form a strong, stable collagen fibrils and fibers that provides strength, integrity and structure. Among 20 different collagen types, I and III are synthesized in huge amount. Collagen type I is stronger, mature and thick whereas type III is less cross-linked and immature that provides less tensile strength predominantly found in early wound healing [29]. Balanced collagen maturation and degradation by matrix metalloproteinases [64] to form type I collagen is a requirement for normal scar formation [29, 30]. Reduced ratio of collagen type I to III lead to thinner collagen fibrils, changed geometrical arrangement [37] with higher levels of non-polymeric soluble collagen [29] that contributes to a decreased tensile strength and instability of the connective tissue and induced scar tissue [11].

It has been proven that the fibroblastic ingrowth, chronic inflammation and scar formation is dependent on the weight and structure of the implanted mesh [12, 40, 46, 63, 70], but the quality and mechanics of such scar tissues are characterized by the extent of collagen type I/III [11, 67]. Studies on the ECM of the explanted hernia meshes constructed from PP, polyester and ePTFE shows lowered collagen

type I/III and reduced tensile strength, a major reason for hernia recurrence [41]. Though, altered ratios of collagen can be seen within fibroblasts located at the edges of recurrent hernia [50], yet it is not clear if the type of mesh used has any effect [12].

Mesh Wrinkling

Wrinkling of the mesh is caused by failure or inadequate mesh fixation in defected place. In the sutureless technique to repair abdominal hernia, meshes are placed flat on the floor of the abdomen. With insufficient dissection to insert the meshes, during physiological movement, meshes have a tendency to wrinkle or curl increasing the potential for the formation of dead spaces where unintended mesh overlap occurs, see Fig. 10a. This process augments the mesh relative movement from its total implanted position leaving gaps at the edges for the protrusion of tissues, causing hernia recurrence, see Fig. 10b. Further, the localized fibroblastic infiltration into mesh pores are greatly altered that mechanically cause inhomogeneous inelastic mesh deformation between the implant (stiffer scar tissue around mesh at dead spaces) and the underlying soft tissue and biologically (a) leaves spaces for infection, (b) chronic postoperative pain, and mesh deterioration. A wrinkled mesh may also add to adhesion problems with viscera which can result in the uneven distribution of stress on the mesh and cause an undesirable distortion, premature weakening of the mesh, and hence predispose the wound to infection [82].

Other reasons of wrinkling have been identified due to (a) tearing edge fibers out of seam during mechanical loadings, (Fig. 7b) and (b) extreme pore deformation (Figs. 6a, b and 7c). Surgeons often cut the desired dimension of the mesh out of a large flat sheet to match the defect to be repaired; edge fibers loosely supported along the transverse woven direction get pulled out when the mesh is stretched. The fibers once out of the knitted mesh can no longer maintain their flat shape and start to curl around. In addition, pores of the compliant meshes can completely collapse under uniaxial mesh stretch. This process dramatically curls the mesh into an unclosed cylindrical geometry from its initial flat shape, see Fig. 6a, b. Repeated

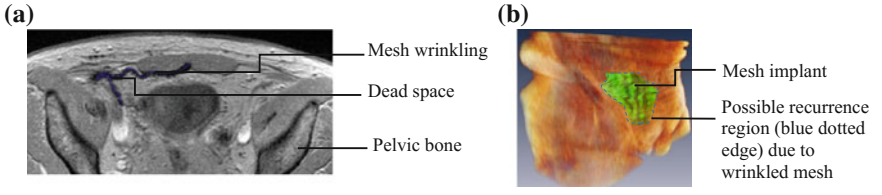

Fig. 10 *Segmentation with* Amira® (Zuse Institute Berlin, *FEI™ Bordeaux*) of *a*bdominal hernia repair using mesh implant [34]: **a** MRI image showing mesh wrinkled after placed in the abdomen: superior view (with permission of N. A. Krämer, Uniklinik RWTH Aachen, Germany); **b** representation of the position of the wrinkled mesh in abdomen (anterior-lateral view)

loading and unloading during rest and straining damages the ingrown tissue, impairing the mechanical biocompatibility of the implantation and finally recurring the damage. A physiologically relevant preconditioning prior to implantation might suppress such mesh wrinkling, but a hypothetic preconditioning procedure might make the mesh less compliant than initially expected.

Mesh Shrinkage

Shrinkage is most common in the surgical repair with the use of heavyweight small pore size PP meshes. Studies assume that it is not the mesh which undergoes shrinkage [50], which is supported by our strain measurement on mesh implants. Assuming the thickness of the mesh to remain constant during test, the mesh area increases on stretching, see Fig. 11. Mesh shrinkage results due to contraction of scar tissue around the mesh, starting with a constant water loss, followed by a surface area decrease [2]. Depending on the properties (pore size, weight and filament type) of the prosthesis, shrinkage of the mesh implants due to wound contraction are observed to be within a wide range from 5–62% [39, 50, 75]. Therefore, use of large implants to cover defects can justify the shrinkage effect, however, larger foreign body reactions, scarring, dyspareunia, shrinkage, mesh exposure and stiffening of the recipient host tissue can no longer be avoided [59]. Lightweight large porous PP meshes are specifically designed to reduce the bridging and scar formation [45], however, the use of highly inert PVDF material is found to significantly reduce the wound contraction, (9.3–19.9%) minimal loss of the original area [22, 39] provide long-term stability as a result of lower foreign body reaction and maintain original strength after years of implantation [32, 45, 49].

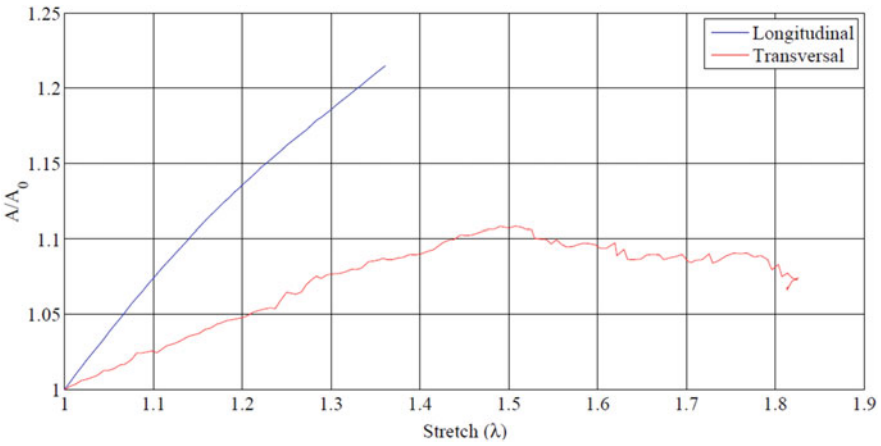

Fig. 11 Area change under uniaxial tensile test on SIS direct soft mesh. A_0 and A are the initial and current surface area of the mesh

Pain

Biomaterials, such as mesh implants are associated with a potential risk of chronic pain, as they are recognized as foreign body by the host tissue immediately after repair. The reasons for chronic pain are still unclear and vary from patient to patient. Studies suggest pain associated with mesh surgery can be (a) early pain immediately after surgery due to irritation from surgical material or nerve damage during surgery or (b) chronic pain existing for more than 3 months after surgery [50]. Repairs using small pore, heavyweight meshes with reduced effective porosity lead mainly to complaints about chronic pain that often requires the complete removal of the implant from the body [53, 69]. Post-retrieval studies on such explants obtained from similar patients with failed repair indicate irritation and destruction of nerve fiber and fascicles by the inflammation at the interface with the mesh [50]. Today's new generation meshes have been greatly improved using softer material, large pore and light weight meshes [44] which have proved to be a better mesh material with reduced level of inflammation and scar formation, which is directly related to pain [70].

Infection

Infection is another common FBR in repair using mesh implants, hindering the local clearance from bacteria [15]; Klinge and Klosterhalfen, 2002 that leads to a chronic inflammatory wound with marked scarring, loss of compliance, mesh contraction, migration, physiochemical changes, seroma, and in some cases, eventual mesh removal to resolve the problem [55]. The incidence of chronic mesh infection is highly related to the type of mesh material, type of filament, pore size, and porosity [23, 70]. Generally, microporous and multifilament meshes with increased surface of the mesh area and small pores are at higher risk of infection than large porous monofilament meshes (>75 μm). Macrophages and neutrophils are unable to enter small pores (<10 μm) but allows bacteria (<1 μm) to survive unchallenged within the pores. In contrast, there is some evidence that the persistence of the (a) colonies of Staphylococcus epidermis bacteria at the surface of the polymer fibers [50], and (b) acute/chronic inflammatory response beyond a 3 weeks period usually indicate higher risk of infection [5]. Chronic mesh infection following repair with small pore meshes or film like structures often requires removal of the infected mesh, which rarely results in hernia recurrence if sufficient fibrosis scarring remains [2]. Open pore meshes mostly can be treated conventionally.

3.7.2 Discussions

A physiological process of wound healing creates a combined reparative layer of implant and fat or connective tissue, which is assumed to be achieved from meshes with sufficient pore dimension and minimum surface area. Small pore sized mesh

intensifies the fibrosis forming thicker scar tissue with poor or no fat cell penetration to the pore. Mechanical response of such heterogeneous neo-scar tissue hugely differs from the anisotropic recipient host tissue that may increase the risk of infection, chronic pain, complete removal of the implant from the body, and recurrence. Under extreme physiological movements and straining processes, higher tensile and shear stresses on the ingrown tissue develops, which increase the risk of postoperative complications such as mesh wrinkling and mesh erosion. Moreover, if mesh pores are heavily deformed and wrinkling of the mesh occurs (Fig. 5b, c), large stresses are developed at the edges of the interface (Fig. 6c). During this process, the implanted mesh may wrap the host tissue and comes in contact with the adjacent organs to irritate, degenerate and even lead to dysfunction of the organs.

Specimen, during surgery, constructed by cutting the desired dimension out of a large flat sheets to repair the defects often leaves free edges that gets seam out when it is stretched. The fibers once pulled out of the knitted mesh can no longer maintain their flat shape and start to stress the tissue locally. Successive tearing further debonds the ingrown tissue and the implanted mesh fails to perform the intended task in the body, see Fig. 6b. Repeated loading and unloading during rest and straining damages the ingrown tissue, impairing the mechanical biocompatibility of the implantation and finally recurring the damage. Thus, adequate structural stability as shown in Fig. 6a, which preserves the porosity under strain is essential for the proper function of such textile structures in a tensile environment in vivo.

The common trend in clinical practice for the reconstructive surgery has been the use of monofilamentous, lightweight large porous mesh in order to reduce the foreign body reaction and to minimize the risk of complications. Soft meshes with an adequate textile construction preserve their effective porosity and show structural stability under mechanical strain and lead to reduced scar formation. However, compliant meshes with additive softer material are often associated with intense pore deformation reducing the effective porosity [19, 36], therefore, a good compromise of the mesh stiffness (formstability), polymer type and pore size should be maintained. Rigorous clinical trials of such mesh should be done with respect to the deposition of physiologically regenerated tissue, for example, fat with the amount of stromal and fibroblasts, percentage of apoptotic cells, degree of foreign body response to compare the effectiveness of the available implants. This not only improves the behavior of existing meshes but insights to search for biomaterials with perfect biocompatibility in order to develop the ideal textile devices which can mimic the biomechanical properties of the tissues.

Calculation of the shear stress and maximum principal stresses at the tissue-implant interface and the estimation of change of the structural proteins after implantation could be quantities to compare the effectiveness of the meshes for such reconstructive surgeries. Depending on the geometry of the pore, mesh orientation and the loading direction, the physiological deformation of the implanted large pore mesh is beneficial if these stresses can be minimized and if adjacent tissue degeneration is successively avoided.

In conclusion, this study shows that meshes with appropriate pore geometry, adequate biaxial stiffness lead to a mechanically biocompatible structure during complex physiological conditions compared to conventional mesh geometry. Since the immune response and repair functions in the body are so complicated, it is not adequate to describe the biocompatibility of a single material in relation to a single tissue surrogate gelatin. However, these tests constitute an important step towards the laboratory animal testing and clinical trials that will determine the biocompatibility of the different meshes with variation in pore geometry, structure and material composition in a given application. Considering these shortcomings, the perfect mesh design should consider sufficient tensile strength, anisotropy/isotropy, elasticity, and provide the appropriate biomimetic environment to ensure cell survival and at the same time should preserve its porosity under strain.

Acknowledgements The first author has been partially funded by the German Federal Ministry of Education and Research through the FHprofUnt project BINGO (03FH073PX2). We would also like to thank our project partner FEG Textiltechnik mbH, Aachen, Germany for providing the prostheses, Nils Andreas Krämer, PD MD, Uniklinikum RWTH Aachen, Germany for providing MRI data, and Andreas Horbach, DI, and our students Christian Halbauer, Viola Gruben for their help with experiments and providing the results from their bachelor theses. The authors would also like to acknowledge Prof. Dr. Melinda Harman, Clemson University for providing permission to use the images reprinted in Fig. 9.

References

1. Alaedeen, D. I., Lipman, J., Medalie, D., & Rosen, M. J. (2007). The single staged approach to the surgical management of abdominal wall hernias in contaminated fields. *Hernia, 11*(1), 41–45.
2. Amid, P. K. (1997). Classification of biomaterials and their related complications in abdominal wall surgery. *Hernia, 1*(1), 15–21.
3. Amid, P. K. (2004). Shrinkage: fake or fact? In V. Schumpelick & L. M. Nyhus (Eds.), *Meshes: benefits and risks*. Berlin: Springer.
4. Anderson, J. M. (1988). Inflammatory response to implants. *ASAIO Transactions, 34*(2), 101–107.
5. Anderson, J. M., Rodriguez, A., & Chang, D. T. (2008). Foreign body reaction to biomaterials. *Seminars in Immunology, 20*(2), 86–100.
6. Anurov, M. V., Titkova, S. M., & Oettinger, A. P. (2012). Biomechanical compatibility of surgical mesh and fascia being reinforced: Dependence of experimental hernia defect repair results on anisotropic surgical mesh positioning. *Hernia, 16*(2), 199–210.
7. Arshady, R. (2003). Polymeric biomaterials: chemistry, concepts, criteria. In R. Arshady (Ed.), *Introduction to polymeric biomaterials: the polymeric biomaterials series* (pp. 1–62). London: Citus Books.
8. Baktir, A., Dogru, O., Girgin, M., Aygen, E., Kanat, B. H., Dabak, D. O., et al. (2013). The effects of different prosthetic materials on the formation of collagen types in incisional hernia. *Hernia, 17*(2), 249–253.
9. Bay-Nielsen, M., Kehlet, H., Strand, L., Malmstrøm. J., Andersen, F. H., Wara, P. et al. (2001). Quality assessment of 26,304 herniorrhaphies in Denmark: A prospective nationwide study. *Lancet, 358*(9288), 1124–1128.

10. Bendavid, R., & Kux, M. (2001). Seromas. In R. Bendavid, J. Abrahamson, M. E. Arregui, J. B. Flament, & E. H. Phillips (Eds.), *Abdominal wall hernias: Principles and management* (pp. 753–756). New York: Springer.
11. Birk, D. E., Fitch, J. M., Babiarz, J. P., Doane, K. J., & Linsenmayer, T. F. (1990). Collagen fibrillogenesis in vitro: interaction of types I and V collagen regulates fibril diameter. *Journal of Cell Science, 95*(Pt 4), 649–657.
12. Brown, C. N., & Finch, J. G. (2010). Which mesh for hernia repair? *Annals of the Royal College of Surgeons of England, 92*(4), 272–278.
13. Brown, G. L., Richardson, J. D., Malangoni, M. A., Tobin, G. R., Ackerman, D., & Polk, H. C. (1985). Comparison of prosthetic material for abdominal wall reconstruction in the presence of contamination and infection. *Annals of Surgery, 201*(6), 705–711.
14. Burger, J. W. A., Luijendijk, R. W., Hop, W. C. J., Halm, J. A., Verdaasdonk, E. G., & Jeekel, J. (2004). Long-term follow-up of a randomized controlled trial of suture versus mesh repair of incisional hernia. *Annals of Surgery, 240*(4), 578–585.
15. Casey, E. M. (2015). *Physical characterization of surgical mesh after function in hernia repair* (*Master Thesis*). Clemson University, South Carolina, USA. All Theses. Paper 2085.
16. Chen, E. H., Grote, E., Mohler, W., et al. (2007). Cell-cell fusion. *FEBS Letters, 581*(11), 2181–2193.
17. Choe, J. M., Kothandapani, R., James, L., & Bowling, D. (2001). Autologous, cadaveric, and synthetic materials used in sling surgery: comparative biomechanical analysis. *Urology, 58*(3), 482–486.
18. Chuback, J. A., Singh, R. S., Sills, C., & Dick, L. S. (2000). Small bowel obstruction resulting from mesh plug migration after open inguinal hernia repair. *Surgery, 127*(4), 475–476.
19. Ciritsis, A., Horbach, A., Staat, M., Kuhl, C. K., & Kraemer, N. A. (2018). Porosity and tissue integration of elastic mesh implants evaluated in vitro and in vivo. *Journal of Biomedical Materials Research Part B: Applied Biomaterials*. 106(2):827–833.
20. Cobb, W. S., Burns, J. M., Peindl, R. D., Carbonell, A. M., Matthews, B. D., Kercher, K. W., et al. (2006). Textile analysis of heavy-weight, mid-weight and light-weight polypropylene mesh in a porcine ventral hernia model. *Journal of Surgical Research, 136*(1), 1–7.
21. Cobb, W. S., Kercher, K. W., & Heniford, B. T. (2005). The argument for lightweight polypropylene mesh in hernia repair. *Surgical Innovation, 12*(1), 63–69.
22. Conze, J., Junge, K., Weiss, C., Anurov, M., Oettinger, A., Klinge, U., et al. (2008). New polymer for intra-abdominal meshes-PVDF copolymer. *Journal of Biomedical Materials Research. Part B, Applied Biomaterials, 87(2),* 321–328.
23. Deligiannidis, N., Papavasiliou, I., Sapalidis, K., Kesisoglou, I., Papavramidis, S., & Gamvros, O. (2002). The use of three different mesh materials in the treatment of abdominal wall defects. *Hernia, 6(2),* 51–55.
24. Dietz, H. P., Vancaillie, P., Svehla, M., Walsh, W., Steensma, A. B., & Vancaillie, T. G. (2003). Mechanical properties of urogynecologic implant materials. *International Urogynecology Journal and Pelvic Floor Dysfunction, 14*(4), 239–243.
25. Dương, M. T., Seifarth, V., Artmann, A.. T., Artmann, G. M., & Staat, M. (2018). Growth modelling promoting mechanical stimulation of smooth muscle cells of porcine tubular organs in a fibrin-PVDF scaffold. In G.M. Artmann, I.E. Digel, A. Zhubanova, A. Temiz Artmann (eds.), *Biological, Physical and Technical Basics of Cell Engineering* (pp. 211–234). Singapore: Springer Nature. 10.1007/978-981-10-7904-7_9.
26. Fenner, D. E. (2000). New surgical mesh. *Clinical Obstetrics and Gynecology, 43*(3), 650–658.
27. Feola, A., Barone, W., Moalli, P., & Abramowitch, S. (2013). Characterizing the ex vivo textile and structural properties of synthetic prolapse mesh products. *International Urogynecology Journal, 24*(4), 559–564.
28. Fischer, T., Ladurner, R., Gangkofer, A., Mussack, T., Reiser, M., & Lienemann, A. (2007). Functional cine MRI of the abdomen for the assessment of implanted synthetic mesh in patients after incisional hernia repair: initial results. *European Radiology, 17*(12), 3123–3129.

29. Fleischmajer, R., Perlish, J. S., Burgeson, R. E., Shaikh-Bahai, F., & Timpl, R. (1990). Type I and type III collagen interactions during fibrillogenesis. *Annals of the New York Academy of Sciences, 580,* 161–175.
30. Friedman, D. W., Boyd, C. D., Mackenzie, J. W., Norton, P., Olson, R. M., & Deak, S. B. (1993). Regulation of collagen gene expression in keloids and hypertrophic scars. *Journal of Surgical Research, 55*(2), 214–222.
31. Frotscher, R., & Staat, M. (2014). Stresses produced by different textile mesh implants in a tissue equivalent. *BioNanoMaterials, 15*(1–2), 25–30.
32. Göretzlehner, U., & Müllen, A. (2007). PVDF als Implantat-Werkstoff in der Urogynäkologie. *Biomaterialien, 8*(S1), 28–29.
33. de la Gutiérrez, P. C., Vargas Romero, J., & Diéguez García, J. A. (2001). The value of CT diagnosis of hernia recurrence after prosthetic repair of ventral incisional hernias. *European Radiology, 11*(7), 1161–1164.
34. Halbauer, C. (2014). Charakterisierung und Vergleich des mechanischen Verhaltens von in Gelatine gebetteten Netzimplantaten durch einen Aero-Bulgetest gegenüber einer FEM Simulation sowie die Entwicklung einer auf MRT-Scans basierenden 3D Visualisierungsmethode implantierter Netze. Unpublished bachelor thesis, Aachen University of Applied Sciences, Jülich.
35. Heniford, B. T., Park, A., Ramshaw, B. J., & Voeller, G. (2003). Laparoscopic repair of ventral hernias: Nine years' experience with 850 consecutive hernias. *Annals of Surgery, 238* (3), 391–399.
36. Horbach, A. J., Duong, M. T., & Staat, M. (2017). Modelling of compressible and othotropic mesh implants based on optical deformation measurement. *Journal of the Mechanical Behavior of Biomedical Materials, 74,* 400–410.
37. Hurme, T., Kalimo, H., Sandberg, M., Lehto, M., & Vuorio, E. (1991). Localization of type I and III collagen and fibronectin production in injured gastrocnemius muscle. *Laboratory Investigation, 64(1),* 76–84.
38. Jerabek, J., Novotny, T., Vesely, K., Cagas, J., Jedlicka, V., Vlcek, P., et al. (2014). Evaluation of three purely polypropylene meshes of different pore sizes in an onlay position in a New Zealand white rabbit model. *Hernia, 18*(6), 855–864.
39. Junge, K., Binnebösel, M., Rosch, R., Jansen, M., Kämmer, D., Otto, J., et al. (2009). Adhesion formation of a polyvinylidenfluoride/polypropylene mesh for intra-abdominal placement in a rodent animal model. *Surgical Endoscopy, 23(2),* 327–333.
40. Junge, K., Binnebösel, M., von Trotha, K. T., Rosch, R., Klinge, U., Neumann, U. P., et al. (2012). Mesh biocompatibility: Effects of cellular inflammation and tissue remodelling. *Langenbeck's Archives of Surgery, 397*(2), 255–270.
41. Junge, K., Klinge, U., Rosch, R., Mertens, P. R., Kirch, J., Klosterhalfen, B., et al. (2004). Decreased collagen type I/III ratio in patients with recurring hernia after implantation with alloplastic prostheses. *Langenbeck's Archives of Surgery, 389(1),* 17–22.
42. Klinge, U. (2007). Experimental comparison of monofile light and heavy polypropylene meshes: less weight does not mean less biological response. *World Journal of Surgery, 31*(4), 867–868.
43. Klinge, U., Binnebösel, M., Kuschel, S., & Schuessler, B. (2007). Demands and properties of alloplastic implants for the treatment of stress urinary incontinence. *Expert Review of Medical Devices, 4*(3), 349–359.
44. Klinge, U., & Klosterhalfen, B. (2012). Modified classification of surgical meshes for hernia repair based on the analysis of 1,000 explanted meshes. *Hernia, 16*(3), 251–258.
45. Klinge, U., Klosterhalfen, B., Müller, M., Ottinger, A. P., & Schumpelick V. (1998). Shrinking of polypropylene mesh in vivo: An experimental study in dogs. *European Journal of Surgery, 164*(12), 965–969.
46. Klinge, U., Klosterhalfen, B., Birkenhauer, V., Junge, K., Conze, J., & Schumpelick, V. (2002). Impact of polymer pore size on the interface scar formation in a rat model. *Journal of Surgical Research, 103*(2), 208–214.

47. Klinge, U., Park, J. K., & Klosterhalfen, B. (2013). The ideal mesh? *Pathobiology, 80,* 169–175.
48. Klinge, U., Si, Z. Y., Zheng, H., Schumpelick, V., Bhardwaj, R. S., & Klosterhalfen, B. (2000). Abnormal collagen I to III distribution in the skin of patients with incisional hernia. *European surgical Research, 32*(1), 43–48.
49. Klink, C. D., Junge, K., Binnebösel, M., et al. (2011). Comparison of long-term biocompatibility of PVDF and PP meshes. *Journal of Investigative Surgery, 24*(6), 292–299.
50. Klosterhalfen, B., Junge, K., & Klinge, U. (2005). The lightweight and large porous mesh concept for hernia repair. *Expert Review of Medical Devices, 2*(1), 103–117.
51. Klosterhalfen, B., Klinge, U., & Schumpelick, V. (1998). Functional and morphological evaluation of different polypropylene-mesh modifications for abdominal wall repair. *Biomaterials, 19*(24), 2235–2246.
52. Langer, C., Neufang, T., Kley, C., Liersch, T., & Becker, H. (2001). Central mesh recurrence after incisional hernia repair with Marlex are the meshes strong enough? *Hernia, 5*(3), 164–167.
53. Laroche, G., Marois, Y., Schwarz, E., Guidoin, R., King, M. W., Pâris, E., et al. (1995). Polyvinylidene fluoride monofilament sutures: Can they be used safely for long-term anastomoses in the thoracic aorta? *Artificial Organs, 19*(11), 1190–1199.
54. Law, N. W., & Ellis, H. (1988). Adhesion formation and peritoneal healing on prosthetic materials. *Clinical Materials, 3*(2), 95–101.
55. Leber, G. E., Garb, J. L., Alexander, A. I., & Reed, W. P. (1998). Long-term complications associated with prosthetic repair of incisional hernias. *Archives of Surgery, 133*(4), 378–382.
56. LeBlanc, K. A. (2001). The critical technical aspects of laparoscopic repair of ventral and incisional hernias. *American Surgeon, 67*(8), 809–812.
57. Lehr, S. C., & Schuricht, A. L. (2001). A minimally invasive approach for treating postoperative seromas after incisional hernia repair. *JSLS-Journal of the Society of Laparoendoscopic Surgeons, 5*(3), 267–271.
58. Liang, R., Abramowitch, S., Knight, K., Palcsey, S., Nolfi, A., Feola, A., et al. (2013). Vaginal degeneration following implantation of synthetic mesh with increased stiffness. *British Journal of Obstetrics and Gynaecology, 120*(2), 233–243.
59. Margulies, R. U., Lewicky-Gaupp, C., Fenner, D. E., McGuire, E. J., Clemens, J. Q., & Delancey, J. O. (2008). Complications requiring reoperation following vaginal mesh kit procedures for prolapse. *American Journal of Obstetrics & Gynecology, 199*(6), 678.e1–678.e4.
60. Matthews, B. D., Pratt, B. L., Pollinger, H. S., Backus, C. L., Kercher, K. W., Sing, R. F., et al. (2003). Assessment of adhesion formation to intra-abdominal polypropylene mesh and polytetrafluoroethylene mesh. *Journal of Surgical Research, 114*(2), 126–132.
61. Mohamed, M., Elmoghrabi, A., Shepard W. R., & McCann, M. (2016) Delayed onset seroma formation 'opting out' at 5 years after ventral incisional hernia repair. *BMJ Case Reports 2016*. https://doi.org/10.1136/bcr-2016-215034
62. Morris-Stiff, G. J., & Hughes, L. E. (1998). The outcomes of nonabsorbable mesh placed within the abdominal cavity: literature review and clinical experience. *Journal of the American College of Surgeons, 186*(3), 352–367.
63. Mühl, T., Binnebösel, M., Klinge, U., & Goedderz, T. (2008). New objective measurement to characterize the porosity of textile implants. *Journal of Biomedical Materials Research. Part B, Applied Biomaterials, 84*(1), 176–183.
64. Nagase, H., Visse, R., & Murphy, G. (2006). Structure and function of matrix metalloproteinases and TIMPs. *Cardiovascular Research, 69(3),* 562–573.
65. Orenstein, S. B., Saberski, E. R., Kreutzer, D. L., & Novitsky, Y. W. (2012). Comparative analysis of histopathologic effects of synthetic meshes based on material, weight, and pore size in mice. *Journal of Surgical Research, 176*(2), 423–429.

66. Otto, J., Kaldenhoff, E., Kirschner-Hermanns, R., Mühl, T., & Klinge, U. (2014). Elongation of textile pelvic floor implants under load is related to complete loss of effective porosity, thereby favoring incorporation in scar plates. *Journal of Biomedical Materials Research Part A, 102*(4), 1079–1084.
67. Pans, A., Albert, A., Lapière, C. M., & Nusgens, B. (2001). Biochemical study of collagen in adult groin hernias. *Journal of Surgical Research, 95(2),* 107–113.
68. Patel, H., Ostergard, D. R., & Sternschuss, G. (2012). Polypropylene mesh and the host response. *International Urogynecology Journal, 23*(6), 669–679.
69. Poobalan, A. S., Bruce, J., Smith, W. C., King, P. M., Krukowski, Z. H., & Chambers, W. A. (2003). A review of chronic pain after inguinal herniorrhaphy. *Clinical Journal of Pain, 19*(1), 48–54.
70. Post, S., Weiss, B., Willer, M., Neufang, T., & Lorenz, D. (2004). Randomized clinical trial of lightweight composite mesh for Lichtenstein inguinal hernia repair. *British Journal of Surgery, 91*(1), 44–48.
71. Ratner, B. D., Northup, S. J., & Anderson, J. M. (2004). Biological testing of biomaterials. In B. D. Ratner, F. J. Schoen, & J. E. Lemons (Eds.), *Biomaterials science: an introduction to materials in medicine* (2nd ed., pp. 355–360). San Diego: Elsevier.
72. Rutkow, I. M. (2003). Demographic and socioeconomic aspects of hernia repair in the United States in 2003. *Surgical Clinics of North America,* 83(5), 1045–1051, V–VI.
73. Saad, B., Abu-Hijleh, G., & Suter, U. W. (2003). Polymer biocompatibility assessment by cell culture techniques. In R. Arshady (Ed.), *Introduction to polymeric biomaterials: the polymeric biomaterials series* (pp. 263–299). London: Citus Books.
74. Salamone, G., Licari, L., Agrusa, A., Romano, G., Cocorullo, G., & Gulotta, G. (2015). Deep seroma after incisional hernia repair. Case reports and review of the literature. *Annali Italiani di Chirurgia*, 12:86 (ePub).
75. Scheidbach, H., Tamme, C., Tannapfel, A., Lippert, H., & Köckerling, F. (2004). In vivo studies comparing the biocompatibility of various polypropylene meshes and their handling properties during endoscopic total extraperitoneal (TEP) patchplasty: an experimental study in pigs. *Surgical Endoscopy, 18*(2), 211–220.
76. Schumpelick, V., Conze, J., & Klinge, U. (1996). Preperitoneal meshplasty in incisional hernia repair. A comparative retrospective study of 272 repaired incisional hernias. *Chirurg, 67*(10), 1028–1035.
77. Scott, P. D., Harold, K. L., Craft, R. O., & Roberts, C. C. (2008). Postoperative seroma deep to mesh after laparoscopic ventral hernia repair: computed tomography appearance and implications for treatment. *Radiology Case Reports, 3*(1), art. 10.128.
78. Shoshan, S. (1981). Wound healing. *International Review of Connective Tissue Research, 9,* 1–26.
79. Shoulders, M. D., & Raines, R. T. (2009). Collagen structure and stability. *Annual Review of Biochemistry, 78,* 929–958.
80. Staat, M., Trenz, E., Lohmann, P., Frotscher, R., Klinge, U., Tabaza, R., et al. (2012). New measurements to compare soft tissue anchoring systems in pelvic floor surgery. *Journal of Biomedical Materials Research. Part B, Applied Biomaterials, 100*(4), 924–933.
81. Susmallian, S., Gewurtz, G., Ezri, T., & Charuzi, I. (2001). Seroma after laparoscopic repair of hernia with PTFE patch: is it really a complication? *Hernia, 5(3),* 139–141.
82. Usher, F. C., & Gannon, J. P. (1959). Marlex mesh, a new plastic mesh for replacing tissue defects. *I. Experimental studies. AMA Archives of Surgery, 78*(1), 131–137.
83. Usher, F. C., Ochsner, J., & Jr, Tuttle L. L. (1958). Use of Marlex mesh in the repair of incisional hernias. *American Surgeon, 24*(12), 969–974.
84. van't Riet, M., de Vos van Steenwijk, P. J., Bonthuis, F., Marquet, R. L., Steyerberg, E. W., Jeekel, J., et al. (2003). Prevention of adhesion to prosthetic mesh: comparison of different barriers using an incisional hernia model. *Annals of Surgery*, 237(1), 123–128.

85. Welty, G., Klinge, U., Klosterhalfen, B., Kasperk, R., & Schumpelick, V. (2001). Functional impairment and complaints following incisional hernia repair with different polypropylene meshes. *Hernia, 5*(3), 142–147.
86. Williams, G. T., & Williams, W. J. (1983). Granulomatous inflammation-a review. *Journal of Clinical Pathology, 36*(7), 723–733.
87. Wilson, C. J., Clegg, R. E., Leavesley, D. I., & Pearcy, M. J. (2005). Mediation of biomaterial-cell interactions by adsorbed proteins: a review. *Tissue Engineering, 11*(1–2), 1–18.

Author Biography

Aroj Bhattarai (Nepal) He came from the land of nature. He received his M.Sc. in Computational engineering from the Technical University of Dresden (2010–2012). Since 2013 he joined the Biomechanics Laboratory at Aachen University of Applied Sciences as a Ph.D. candidate. His research (at the Institute of Bioengineering, Biomechanics Laboratory, Aachen University of Applied Sciences) mainly focuses on the finite element method to optimize the surgical repairs of the female pelvic floor dysfunctions using prosthetic mesh implants.